

---

# Upper Stability Island of the Quadrupole Mass Filter with Amplitude Modulation of the Applied Voltages

N. V. Konenkov, A. N. Korolkov, and Marat Machmudov

Ryazan State Pedagogical University, Ryazan, Russia

Modulation of the voltages applied to a quadrupole mass filter (QMF), either RF or RF and DC, leads to splitting of the stability region into islands of stability. The ion optical properties, such as transmission, resolving power and peak tails of the first upper stability islands have been investigated by numerical simulation of ion trajectories. The dependence of the location of this island on the amplitude of the modulation and the parameter  $\nu = \omega/\Omega = Q/P$  where  $\omega$  is modulation frequency,  $\Omega$  is main angular radio frequency, and  $Q$  and  $P$  are integers, is calculated in detail. Different methods of adjusting the QMF resolution are examined. It is found that operation at the upper and lower tips of the stability islands created by amplitude modulation of the RF voltage is preferred, because of the technical simplicity of this method and a reduction of the required separation time. Amplitude modulation improves the performance of a QMF constructed with round rods, in comparison to perfect quadrupole fields. For example, with amplitude modulation of the RF, to reach a resolution of  $R_{0.1} = 1200$  requires only about 75 RF cycles of ion motion in a quadrupole field created by round rods. (J Am Soc Mass Spectrom 2005, 16, 379–387) © 2005 American Society for Mass Spectrometry

---

The resonant excitation of ion oscillations by a weak auxiliary RF signal notably enhances the performance of 3D ion traps [1]. The theory of ion excitation is well-developed and has been applied to the problem of 3D ion trap tandem mass spectrometry [2, 3]. The modulation of the quadrupole mass filter (QMF) voltage,  $U - V \cos \Omega t$ , by a small auxiliary RF signal for resonant excitation of the ion oscillations is discussed in [4]. Data were obtained for the most general case of a periodic trapping voltage, for the 3D ion trap, and for the linear mass filter. The conclusions of that study have not been verified by experiments or by ion trajectory calculations.

Amplitude modulation of the RF and DC potentials applied to a quadrupole is an example of parametric excitation. The theory of parametric resonance of different orders of the ion oscillations in quadrupole RF fields is given in [5] and investigated experimentally in [6]. Mass separation in upper stable island was used previously to modify and improve the peak shape [7]. The general problem of the calculation of stability diagrams for ion motion in periodic RF quadrupole fields is reviewed in [8]. The resonant excitation of the ion oscillations by a weak auxiliary RF signal produces strong changes in the Mathieu stability diagram [5–10]. The excitation causes instability bands, along the iso- $\beta$

lines. As a result, the original stability region splits into islands of stability. Amplitude modulation of the main trapping voltage also produces instability bands on the stability diagram [4, 8].

In this paper we describe a study of the upper stable island caused by modulation of the RF or DC and RF voltages by a small auxiliary signal. The location of the stability islands for different values of the amplitude of modulation and the ratio  $\omega = \omega/\Omega$  are given in detail. Different methods of adjusting the resolution are examined. We show that operation at the upper and lower tips of the islands created by amplitude modulation of the RF voltage is preferred because of the technical simplicity and a reduction of the required separation time. We show that a rod set that is constructed with round rods and operated with modulation of the voltages can give higher performance than an ideal quadrupole field without modulation.

## Methods

Distortions of the quadrupole field are described by the addition of higher spatial harmonics to the potential. In this case the equations of ion motion can be written [11–13] :

$$\frac{d^2x}{d\xi^2} + g(\xi)x = -\frac{1}{2}g(\xi)\sum_{N=3}^{10} \frac{A_N \frac{\partial \Phi_N(x, y)}{\partial x}}{A_2^{N-2}} \quad (1)$$

Published online January 21, 2005

Address reprint requests to Dr. N. V. Konenkov, Department of Physics, Ryazan State Pedagogical University, Sloboda 46, 390000 Ryazan, Russia. E-mail: k@atm.ryazan.ru

$$\frac{d^2y}{d\xi^2} - g(\xi)y = -\frac{1}{2}g(\xi)\sum_{N=3}^{10} \frac{A_N \frac{\partial \Phi_N(x, y)}{\partial y}}{A_2^{N-2}} \quad (2)$$

where  $g(\xi)$  is a function of time,  $\xi = \frac{\Omega t}{2}$ ,  $A_N$  is the dimensionless amplitude of the spatial harmonic of order  $N$ ,  $A_2$  is the amplitude of the main quadrupole harmonic with a value close to 1.00 when field distortions are small [13],  $\Phi_N(x, y) = \text{Re}[(x + iy)^N]$  is the real part of the complex potential function  $(x + iy)^N$ ,  $i = \sqrt{-1}$ , and  $x$  and  $y$  are transverse quadrupole directions.

There are three possible methods of modulating the voltages applied to a quadrupole: (1) amplitude modulation of the RF voltage ( $V \cos \Omega t$ ); (2) amplitude modulation of both the DC and RF voltages ( $U - V \cos \Omega t$ ), (3) amplitude modulation of the DC voltage,  $U$ .

With amplitude modulation at an angular frequency  $\omega$  for case (1), the function  $g(\xi)$  in eqs 1 and 2 is

$$g(\xi) = a - [2q \cos 2(\xi - \xi_0)][1 + m \cos 2v\xi] \quad (3)$$

for case (2)

$$g(\xi) = [a - 2q \cos 2(\xi - \xi_0)][1 + m \cos 2v\xi] \quad (4)$$

and for case (3)

$$g(\xi) = a[1 + m \cos 2v\xi] - 2q \cos 2(\xi - \xi_0), \quad (5)$$

where

$$a = \frac{8eU}{m\Omega^2 r_0^2}, \quad q = \frac{4eV}{m\Omega^2 r_0^2}, \quad v = \frac{\omega}{\Omega} \quad (6)$$

$\xi_0$  is an initial RF phase (phase of ion flight in RF field) and  $m$  is the modulation parameter [6]. Here we consider the first two cases (1) and (2).

With modulation at a rational frequency  $v = \omega/\Omega = M/P$  the instability bands fall on the iso- $\beta$  lines [8]

$$\beta = \frac{k}{P}, \quad k = 1, 2, 3, \dots, P-1 \quad (7)$$

and the solutions of equations of ion motion (eq 1) and (eq 2) in perfect quadrupole field ( $A_2 = 1$  and  $A_N = 0$  for  $N \neq 2$ ) are periodic with period  $\pi P$ . Here we study the ion optical properties of the upper stability island formed by the lines  $\beta_x = (P-1)/P$  and  $\beta_y = 1/P$ .

To calculate the position of an island in the  $a, q$  plane, we use the matrix method [8]. The transmission matrix  $M$  through period  $\pi P$  is

$$\begin{bmatrix} u \\ u' \end{bmatrix} = \begin{bmatrix} m_{11}m_{12} \\ m_{21}m_{22} \end{bmatrix}_{P\pi} \begin{bmatrix} u_0 \\ u'_0 \end{bmatrix} \quad (8)$$

with initial conditions  $u_0 = 1$ ,  $u'_0 = 0$  and  $u_0 = 0$ ,  $u'_0 =$

1. Here  $u = x$  or  $y$  and  $u' = du/d\xi$ . So for  $u_0 = 1$ ,  $u'_0 = 0$  we have

$$\begin{bmatrix} u_1 \\ u'_1 \end{bmatrix} = \begin{bmatrix} m_{11}m_{12} \\ m_{21}m_{22} \end{bmatrix}_{P\pi} \begin{bmatrix} 1 \\ 0 \end{bmatrix} = \begin{bmatrix} m_{11} \\ m_{21} \end{bmatrix} \quad (9)$$

and for  $u_0 = 0$ ,  $u'_0 = 1$  we calculate

$$\begin{bmatrix} u_2 \\ u'_2 \end{bmatrix} = \begin{bmatrix} m_{11}m_{12} \\ m_{21}m_{22} \end{bmatrix}_{P\pi} \begin{bmatrix} 0 \\ 1 \end{bmatrix} = \begin{bmatrix} m_{12} \\ m_{22} \end{bmatrix} \quad (10)$$

Thus  $m_{11} = u_1$  and  $m_{22} = u'_2$  after period  $\pi P$ . These may be calculated by any suitable numerical method for solving the equations of ion motion (eq 1) and (eq 2) through the interval  $\xi = 0 - \pi P$ , for a perfect quadrupole field. If  $m_{11}(a, q) + m_{22}(a, q) = 2$  the point  $a, q$  corresponds to the boundary of a stability island in the  $a, q$  plane. With this method the upper island positions have been calculated for different values of the parameters  $m$  and  $v$ . With small field distortions, the shifts in island positions are negligible and we can calculate the transmission and resolution for comparison with the perfect field case.

A transmission contour (or peak shape),  $T(q)$ , is calculated with direct ion trajectory simulations [11, 12]. For numerical integration of the equations of ion motion we use the Runge-Kutta-Nystrom-Dormand-Prince (RK-N-DP) method of order of 6 with variable step-size integration. The program is written in PASCAL 7 (Program DOPRIN [14]).

The transmission  $T = N_{tr}/N$  determines the fraction of ions transmitted through the quadrupole field;  $N_{tr}$  is the number of ions transmitted through a quadrupole (oscillation amplitudes less than  $r_0$ ) with a length defined by the number of the RF cycles,  $n$ , that ions spend in the field.  $N$  is the number of ions which fall on a circular input aperture with radius  $R = 0.1r_0$ . A parallel input ion beam is used (i.e., initial transverse ion velocities are zero). Initial conditions are 20 fixed initial RF phases  $\xi_0 = 0, \pi/20, 2\pi/20, 3\pi/20, \dots, 19\pi/20$  for 100 randomly distributed points on the input aperture. As a result, one point on a curve  $T(q)$  corresponds to the calculation of  $N = 2000$  ion trajectories. For detailed study of the peak tails, we increase  $N$  up to 12,000 ion trajectories per point  $(a, q)$ . The focusing effects of fringing fields [15, 16] are not considered here.

There are three ways of adjusting the mass resolution: (1) changing the slope of the scan line  $a = 2\lambda q$  at the lower or upper tips of an island; (2) setting the scan line to pass through the center of an island (for maximize transmission) and changing the modulation parameter  $m$  (sweeping the amplitude of the auxiliary RF signal); (3) setting the scan line to pass through the center of an island and changing of the parameter  $v$  (frequency sweeping of the auxiliary RF signal). Of these methods, it was found that the preferred mode is amplitude modulation of the RF voltage with adjustment of the resolution by changing of the scan line slope

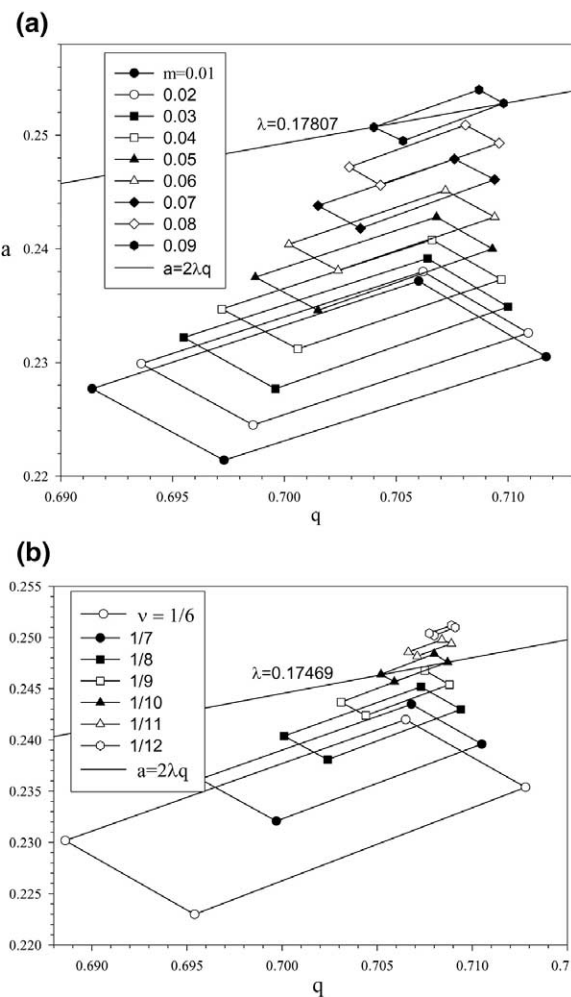


**Figure 1.** Positions of the upper stability islands with amplitude modulation of the RF voltage with different values of the parameters  $m$  and  $\nu$  ( $n = 100$ ,  $N = 2000$ ). (a) Effects of the modulation parameter  $m$  on island position with the frequency ratio  $\nu = 1/8$ . (b) Effects of the value of the frequency ratio  $\nu$  on island position with modulation parameter  $m = 0.06$ .

at the lower or upper tips of chosen stability island, with a low ratio  $\nu = \omega/\Omega$ . This method removes peak tails and requires less separation time ion the mass filter for a given resolution. Direct ion trajectory simulations confirm the validity of the matrix method for calculation of the positions of stability islands in the  $a$ ,  $q$  plane.

## Results and Discussion

### Amplitude Modulation of the RF Voltage

The positions of the upper stability islands in the  $a$ ,  $q$  plane with amplitude modulation of the RF voltage are shown in Figure 1. The stability islands with  $\nu = 1/8$  and for different values of the modulation parameter  $m$  in the range 0.01–0.09 are given in detail in Figure 1a. Matrix elements  $m_{11}$  and  $m_{22}$  were determined by integration on the interval  $0-8\pi$ . The islands have the form of quadrangles with boundaries, which are ap-

proximately straight lines. The instability bands which form the upper stability island follow the iso- $\beta$  lines  $\beta_x = 7/8$  and  $\beta_y = 1/8$  of the original diagram. Increasing the modulation parameter  $m$  decreases the area of an island, and the island moves towards higher values of  $q$  and  $a$ . At the given ratio  $\nu = 1/8$ , a relatively large value of  $m$  is required to reach high resolution (small area). The scan line  $a = 2\lambda q$  with  $\lambda = 0.17807$  crosses the center of the island with parameters  $m = 0.09$  and  $\nu = 1/8$ . The effect of the ratio  $\nu$  in the range 1/6–1/12 on the location of stability islands, with modulation parameter  $m = 0.06$ , is shown in Figure 1b. Decreasing the value  $\nu$  decreases the island area and the islands shift to higher values of  $q$  and  $a$ . At  $\nu = 1/12$  the island splits from the original stability diagram along the  $\beta_x = 11/12$  and  $\beta_y = 1/12$  iso- $\beta$  lines. The width of the instability band increases substantially when the relative frequency  $\nu$  tends to zero.

The transmission and resolution when a scan line crosses the center of the stability islands is illustrated in Figure 2. The transmission contours  $T(q)$  are shown in Figure 2a for different modulation parameters  $m =$

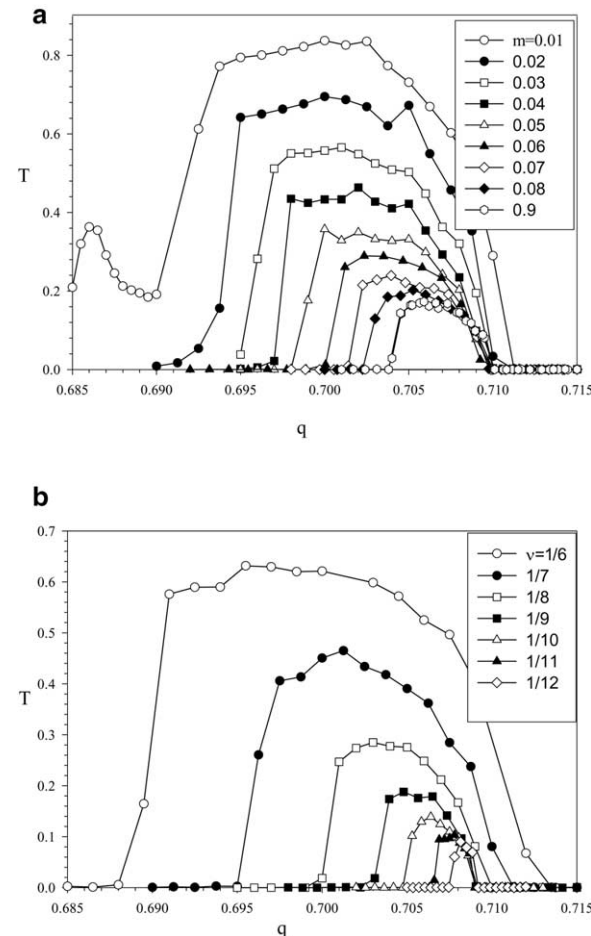


**Figure 2.** Transmission curves  $T(q)$  with an ideal quadrupole field when a scan line  $a = 2\lambda q$  crosses the center of a stability island ( $n = 100$ ,  $N = 2000$ ). (a)  $\nu = 1/8$  and  $m = 0.01-0.90$  (islands of Figure 1a). (b)  $m = 0.06$  and  $\nu = 1/6-1/12$  (islands of Figure 1b).

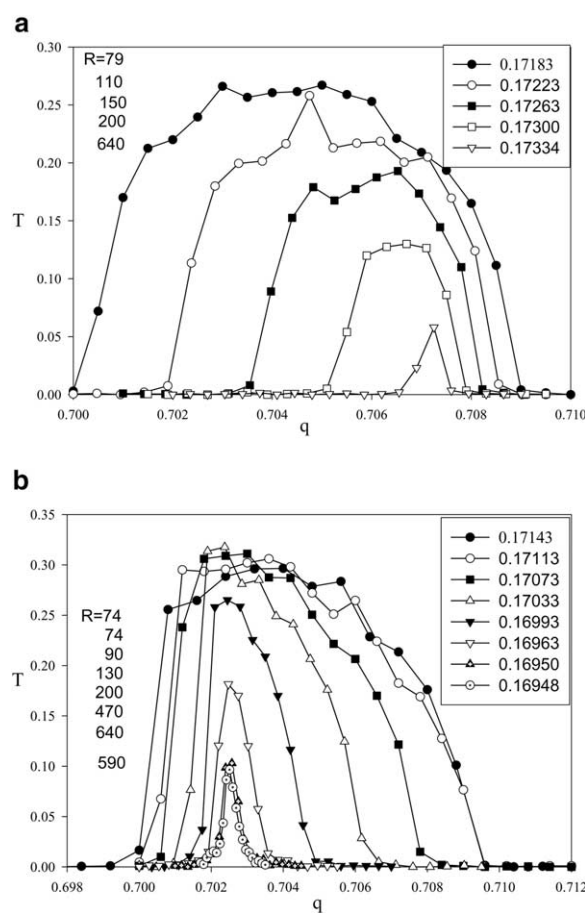


**Figure 3.** Transmission contours  $T(q)$  ( $n = 100$ ,  $N = 2000$ ) with an ideal quadrupole field when a scan line  $a = 2\lambda q$  crosses the stability island with  $\nu = 1/8$  and  $m = 0.06$  at (a) the upper tip and (b) the lower tip.

0.01–0.09 at the ratio  $\nu = 1/8$ . Every curve,  $T(q)$ , corresponds to a scan line which crosses the center of a stability island shown in Figure 1a. With increasing modulation, the peaks shift to higher  $q$  values. At  $m = 0.09$  the tail on the low  $q$  side is less than at  $m = 0.02$  and the resolution is about  $R = 120$  for the same separation time ( $n = 100$ ). The ion trajectory simulations confirm the calculated locations of the stability islands. Figure 2b shows the peaks for the case when the scan line  $a = 2\lambda q$  crosses the center of islands with different values of  $\nu$  (the islands of Figure 1b). Decreasing the ratio  $\nu$  shifts the peaks along the  $q$  axis and decreases the peak width  $\Delta q$ . At  $m = 0.06$  and  $\nu = 1/12$  the tail on the low  $q$  side is eliminated and for the same separation time,  $n = 100$ , there is higher resolution.

Consider the changes of the transmission and resolution with scan parameter  $\lambda = a/2q = U/V$  at the lower and upper tips of a stability island with given  $m$  and  $\nu$ . The transmission contours  $T(q)$  for the island with  $m = 0.06$  and  $\nu = 1/8$  (see Figure 1) with operation at the upper tip are shown in Figure 3a. The resolution values  $R_{<0.1}$ , defined at a level close to zero transmission, are marked on the figure. Good peak shape with

small tails at relatively high resolution  $R = 640$  and small separation time,  $n = 100$ , can be seen. With increasing resolution  $R$ , the peaks shift along the  $q$  axis as expected from the island geometry. The transmission curves for operation at the lower tip of the island with  $m = 0.06$  and  $\nu = 1/8$  (Figure 1b) are shown in Figure 3b. In comparison with operation at the upper tip at resolution  $R = 640$  and  $n = 100$ , tails are formed on the peaks. Thus operation at the upper tip is preferred because it eliminates peak tails.

Higher resolution was obtained with  $m = 0.06$  and  $\nu = 1/12$  (Figure 1b) with a scan line that crosses the island near the upper (Figure 4a) and lower (Figure 4b) tips. The data of Figure 4a show that the transmission  $T$  drops only about a factor of 1.5 as the resolution increases from  $R = 470$  to 2080. This contrasts with conventional operation of a quadrupole where the transmission decreases approximately as  $R^{-1}$  [17], which would give a decrease by a factor of 4.4 for this increase in resolution. A resolution of  $R = 2080$  can be obtained with a separation time of only 100 RF cycles. With operation at the lower tip of the stability island with  $\nu = 1/12$  it is possible to reach a resolution of  $R = 2800$  with  $n = 100$  (Figure 4b).

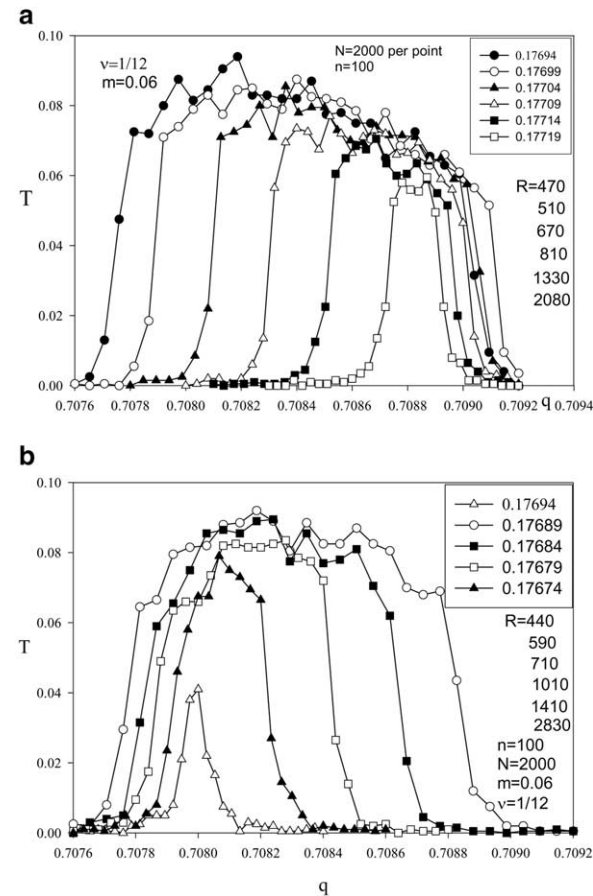


**Figure 4.** High resolution peak shapes with the island with  $m = 0.06$  and  $\nu = 1/12$  ( $n = 100$ ,  $N = 2000$ ). (a) Upper tip (b) lower tip.

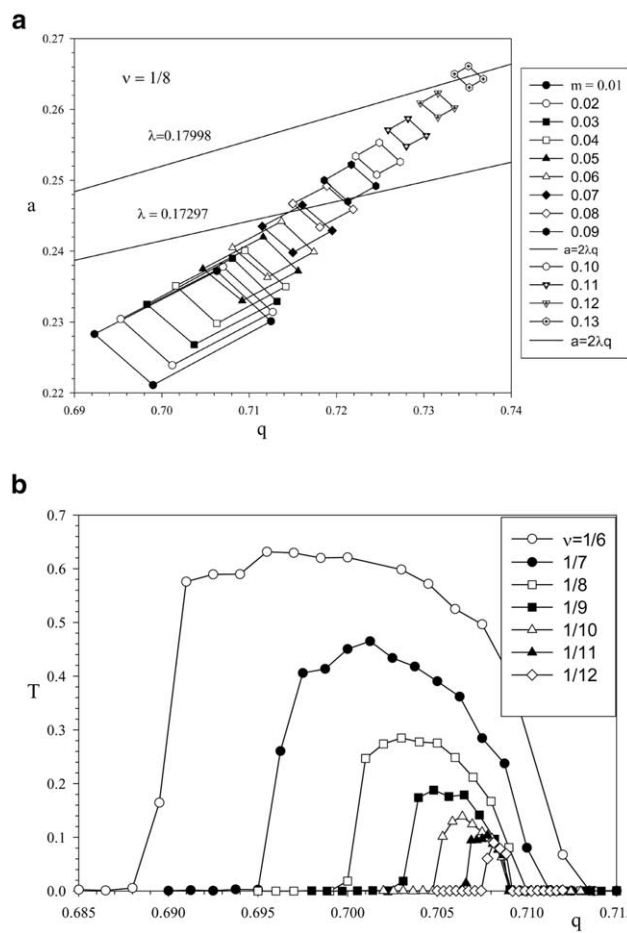


**Figure 5.** Positions of the stability island with amplitude modulation of both the DC and RF voltages for different parameters  $\nu$  and  $m$  ( $n = 100$ ,  $N = 2000$ ). (a)  $\nu = 1/8$  and  $m = 0.01$  to  $0.13$ , (b)  $m = 0.06$  and  $\nu = 1/5, 1/6, \dots, 1/13$ .

### Amplitude Modulation of the RF and DC Voltages

Here we consider the case when both the RF and DC voltages,  $U - V \cos \Omega t$ , are modulated by a small RF signal  $V' \cos \omega t$  (eq 4). The locations of the stability islands at the ratio  $\nu = 1/8$  for modulation parameters  $m$  in the range 0.01–0.13 are given in Figure 5a. With increasing values of  $m$ , the stability islands move to higher  $q$  and  $a$  values. This is similar to the case of amplitude modulation of the RF voltage (Figure 1a), but the island areas are smaller and the islands move to higher  $q$  values. The scan lines  $a = 2\lambda q$ , which cross the center of the islands, require greater changes in  $\lambda$  with increasing modulation parameter  $m$ .

The locations of the stability islands in the  $a$ , $q$  plane for  $m = 0.06$  and  $\nu = 1/6$ – $1/13$  are shown in Figure 5b. The parameter  $\nu$  has a greater effect on the position of the stability islands than the modulation parameter  $m$  (Figure 5b). The scan line  $a = 2\lambda q$  with  $\lambda = 0.15949$ , which crosses a center of the stability island with  $m = 0.06$  and  $\nu = 1/5$ , is shown on this figure. The islands are different from those with amplitude modulation of the RF alone (Figures 1 and 2).

The peak shapes  $T(q)$  when a scan line  $a = 2\lambda q$  crosses the center of the stability islands of Figure 5a are shown in Figure 6a. With increasing values of  $m$ , the peaks shift substantially along the  $q$  axis up to  $q = 0.735$  and the resolution  $R = q/\Delta q$  increases. The transmission  $T$  decreases relatively weakly and the peak tails are eliminated. The low mass side of the peak is sharper than the high mass side. Transmission curves  $T(q)$  for  $m = 0.06$  and different values  $\nu = 1/5$ – $1/11$  when the scan line  $a = 2\lambda q$  crosses the centers of the stability islands are shown in Figure 6b. Again the low mass side of the peak is sharper than the high mass side.

With amplitude modulation of the DC and RF voltages the resolution can also be adjusted by changing the slope of a scan line that passes through the upper or lower tips of an island. Figure 7 shows this for the stability island with  $\nu = 1/8$  and  $m = 0.1$ . The peaks  $T(q)$  with operation at the upper tip are shown in Figure 7a, for different values of  $\lambda$ . There is a symmetric peak shape, but with increasing resolution, peak tails are formed on the high mass side. For the same island, the

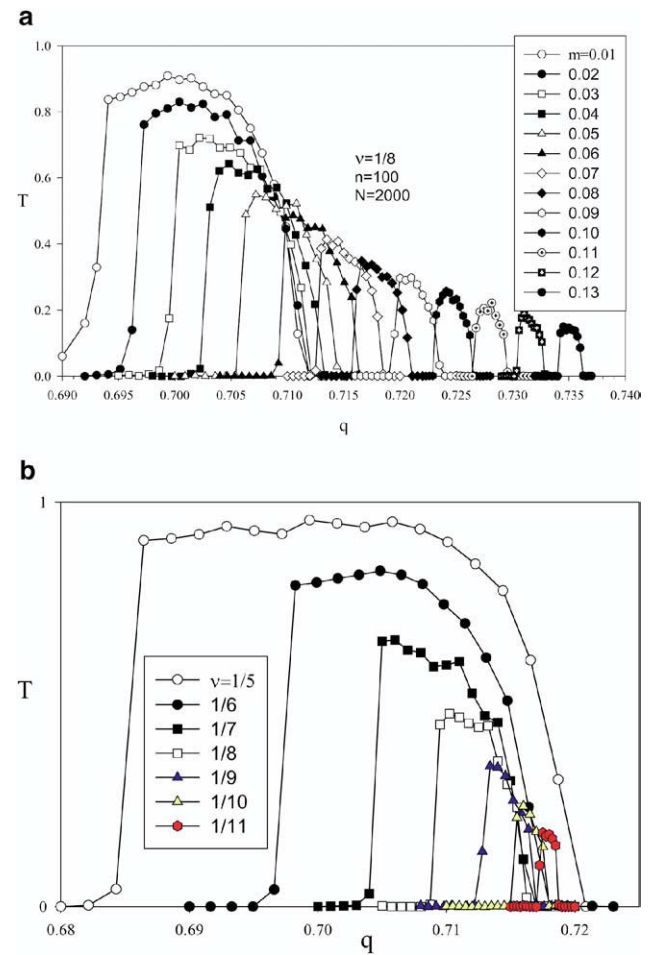


**Figure 6.** Transmission curves  $T(q)$  for an ideal quadrupole field when a scan line  $a = 2\lambda q$  crosses the center of the stability island ( $n = 100$ ,  $N = 2000$ ). (a)  $\nu = 1/8$  and  $m = 0.01$  to  $0.13$  (islands of Figure 5a). (b)  $m = 0.06$  and  $\nu = 1/5, 1/6, \dots, 1/11$  (islands of Figure 5b).

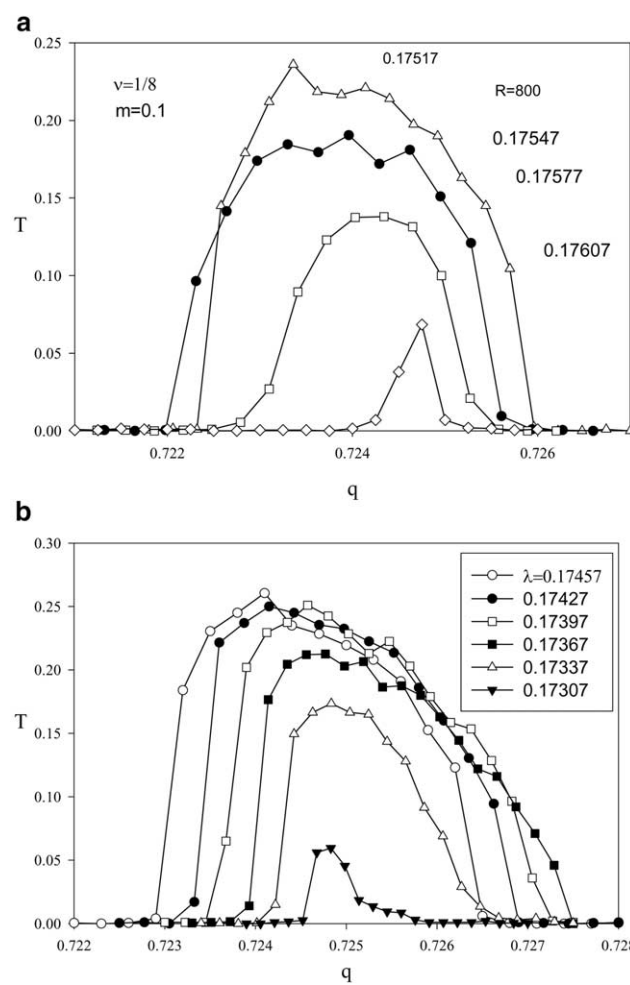


**Figure 7.** Peak shapes for an ideal quadrupole field with modulation of both the RF and DC for the stability island with  $\nu = 1/8$  and  $m = 0.1$  for different scanning parameters  $\lambda$  ( $n = 100$ ,  $N = 2000$ ). (a) Upper tip and (b) lower tip.

curves,  $T(q)$ , for operation at the lower tip are shown in Figure 7b. Increasing resolution leads to formation of a peak tail on the high mass side of the peak. With modulation of both the DC and RF voltages there are sharp peak edges when the scan line crosses the island boundaries formed from iso- $\beta_x$  lines. The boundaries formed from iso- $\beta_y$  lines give low or high mass side tails on the peak with operation at the upper and lower tips respectively.

For the low frequency ratio  $\nu = 1/12$ , and with modulation parameter  $m = 0.06$ , the peak shapes with operation at the upper and lower tips are shown in Figure 8a and b, respectively. With increasing resolution peak tails are formed on the low  $q$  side with operation at the upper tip and on the high  $q$  side with operation at the lower tip of the island. Again, peak tails are formed when the scan line crosses a  $y$  boundary. These peak tails can be removed by increasing the separation time,  $n$ , but this is not always possible in practice.

### Separation Time Effects on Peak Tails and Resolution

The effects of the separation time,  $n$ , on peak shape for the island with  $m = 0.06$  and  $\nu = 1/12$  with RF modulation are illustrated in Figure 9a (operation at the upper tip) and Figure 9b (operation at the lower tip). An ideal quadrupole field was modeled. Increasing the number of RF cycles which ions spend in the field leads to improved peak shape and removes the tails. At  $n = 75$  the resolution is  $R = 1200$  and the transmission  $T = 7\%$ . It is not possible to achieve this in a pure quadrupole field without modulation, as we show later (Figure 10).

The peak shape with a perfect field without excitation for different numbers of RF cycles  $n = 50, 75, 100, 150$ , and 200 are shown in Figure 10. To reach a resolution  $R = 390$  without considerable peak tails requires about  $n = 200$  RF cycles for ion separation. Comparing Figures 9 and 10 shows that operation with RF amplitude modulation gives improved resolution at a given separation time  $n$ .

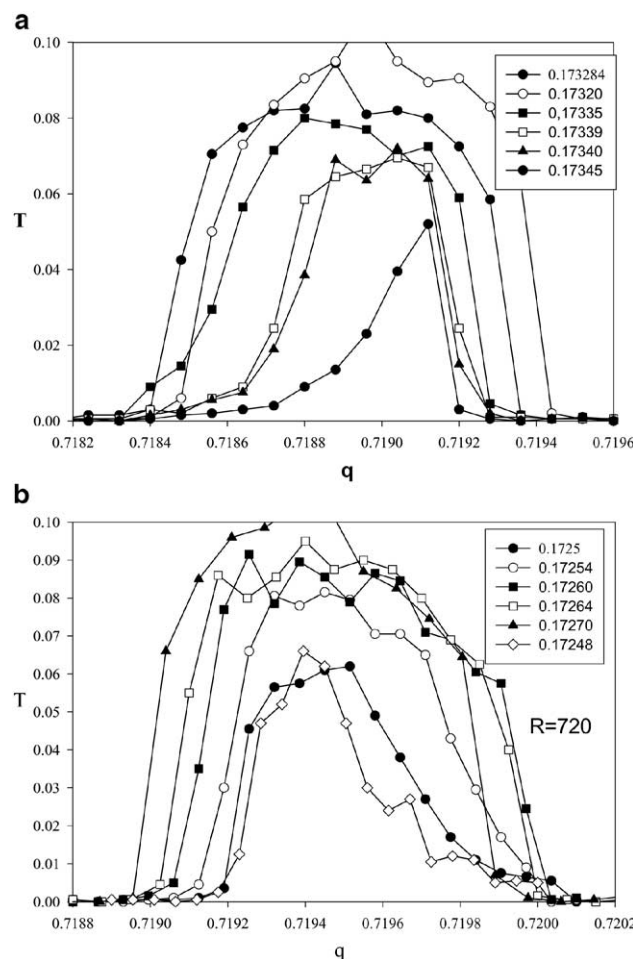


**Figure 8.** Transmission and resolution in the small stability island with modulation of both the RF and DC,  $m = 0.06$ ,  $\nu = 1/12$  and for different scanning parameters  $\lambda$ . Perfect field ( $n = 100$ ,  $N = 2000$ ). (a) Upper tip and (b) lower tip.

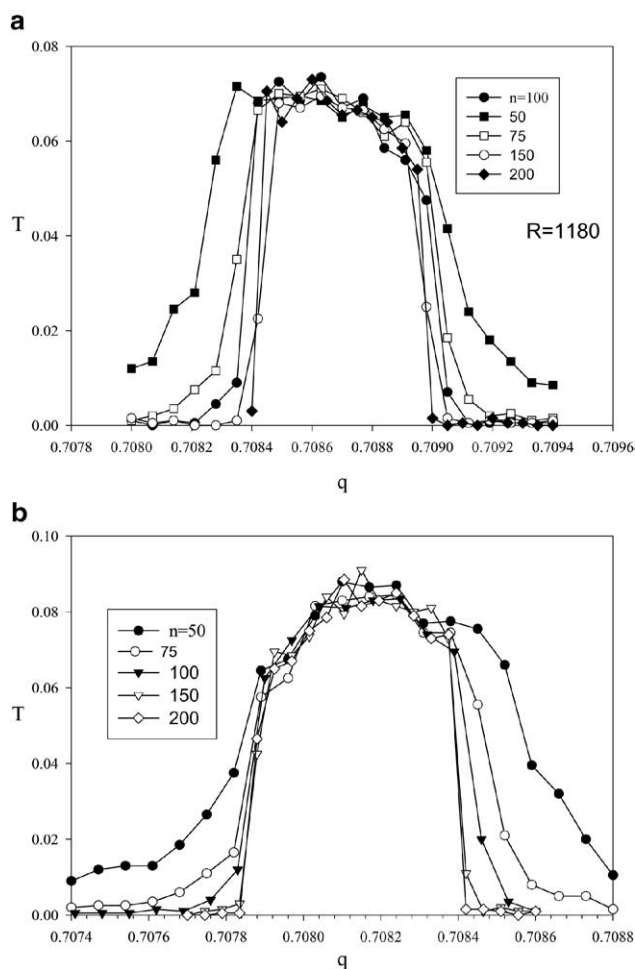


**Figure 9.** Peak shapes for separation times  $n = 50, 75, 100, 150$ , and  $200$ , with operation in the island with  $m = 0.06$  and  $\nu = 1/12$ , amplitude modulation of the RF voltage ( $N = 2000$ ). Ideal quadrupole field. (a) Upper tip,  $\lambda = 0.17711$  and (b) lower tip,  $\lambda = 0.17679$ .

The use of round rods instead of hyperbolic electrodes leads to distortion of the quadrupole field, described by the appearance of additional higher order spatial harmonics in the potential. As a result the low mass side of the peaks have considerable tails. These are minimized at the ratio of rod radius to field radius  $r/r_0 \approx 1.13$  [11] where the effects of the 6th and 10th spatial harmonic compensate each other. For this ratio we calculate transmission curves  $T(q)$  for the case of amplitude modulation of the DC and RF voltages for different values  $n = 50, 75, 100$ , and  $150$  (Figure 11). The effects on peak shape of the separation time for operation with amplitude modulation with parameters  $m = 0.06$ ,  $\nu = 1/11$ , and  $\lambda = 0.17213$  are illustrated in Figure 11a. A separation time  $n = 50$  allows reaching a resolution  $R_{0.1} = 450$  in this mode, with round rods. A value  $n = 150$  is sufficient to remove peak tails at the resolution  $R = 450$ . Figure 11b shows the calculated peak shapes with modulation of the RF only, with  $m = 0.06$ ,  $\nu = 1/12$ , and a scan parameter  $\lambda = 0.1769$ . As with modulation of both the RF and DC, an ion sepa-

ration time of  $150$  RF cycles is sufficient to supply a peak without visible tails. Amplitude modulation with round rods gives peaks with less tailing than a perfect quadrupole field without modulation (Figure 10). However modulation can also be used to remove peak tails with an ideal quadrupole field.

To compare peak shapes over a greater range of transmission, the number of ion trajectories was increased to  $12000$  per point on the curve  $T(q)$ , with the results shown in Figure 12. Curve 1 is the peak shape with a perfect field with  $n = 100$  RF cycles. At low transmission levels the peak is broadened compared to the expected pass band for  $\lambda = 0.1677$ . This is due to the relatively low number of RF cycles,  $n = 100$ . Using round rods with  $r/r_0 = 1.13$  leads to a more intense low mass side peak tail (curve 2) for the same value  $n = 100$ . Transmission curves 2 and 3, respectively, correspond to a distorted field from a rod set with round rods ( $r/r_0 = 1.13$ ), with QMF operation in stability islands with parameters  $m = 0.06$ ,  $\nu = 1/12$ ,  $\lambda = 0.1769$  (modulation of both the DC and RF voltages), and  $m = 0.06$ ,  $\nu = 1/11$ ,  $\lambda = 0.17213$  (modulation of RF voltage only). Figure 12 demonstrates that modulation of the supply voltages offers a method of substantially increasing performance for a round rod set in comparison with a hyperbolic electrode set.

The main conclusion of reference [12], that auxiliary quadrupolar excitation in a perfect field does not improve QMF performance in comparison to a quadrupole without excitation, is not valid, because only low resolution ( $R = 100$ ) was considered in [12]. The data presented here (Figure 12) show that there are improvements in peak shape and resolution with modulation in comparison to a perfect field without modulation.

From a comparison of Figures 10 and 11 we can conclude that to reach a resolution of about  $R_{0.1} = 400$  requires  $n_m = 75$  RF cycles for ion separation with modulation and  $n_q = 150$  without modulation. The axial kinetic ion energy  $E_z$  is related to  $n$  by

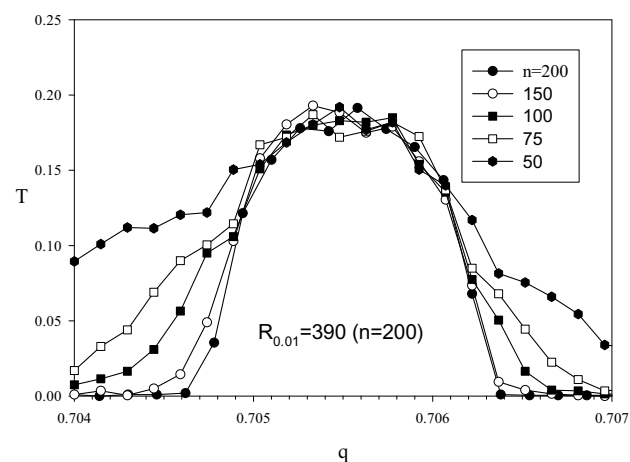


**Figure 10.** Peak shapes with a perfect quadrupole field without modulation for separation times  $n = 50, 75, 100, 150, 200$  with  $\lambda = 0.1676$  ( $q/\Delta q = 390$ ).

$$E_z = \frac{1}{2}mv_z^2 = \frac{1}{2}m\left(\frac{L}{t}\right)^2 = \frac{1}{2}m\left(\frac{Lf}{n}\right)^2 \quad (11)$$

where  $m$  is ion mass,  $v_z$  is the axial ion velocity,  $L$  is the rod length,  $t = nT$  is the flight time of an ion through the quadrupole,  $f = \Omega/2\pi$  is the RF frequency, and  $T$  is the RF period. From eq 11 it follows that for given ion mass and resolution, the ion energy ( $E_z$ )<sub>m</sub> with modulation can be four times higher than for the case of a perfect (and also for a round rod set) quadrupole field:

$$\frac{(E_z)_m}{(E_z)_q} = \left(\frac{n_q}{n_m}\right)^2 \geq 4. \quad (12)$$

This is confirmed by the data of Figure 9 which illustrates relatively high resolution  $R_{0.01} = 1200$  at  $n = 75$ . For effective ion transmission through the fringing field with length  $z_f = 1.5 r_0$ , the time of flight through the

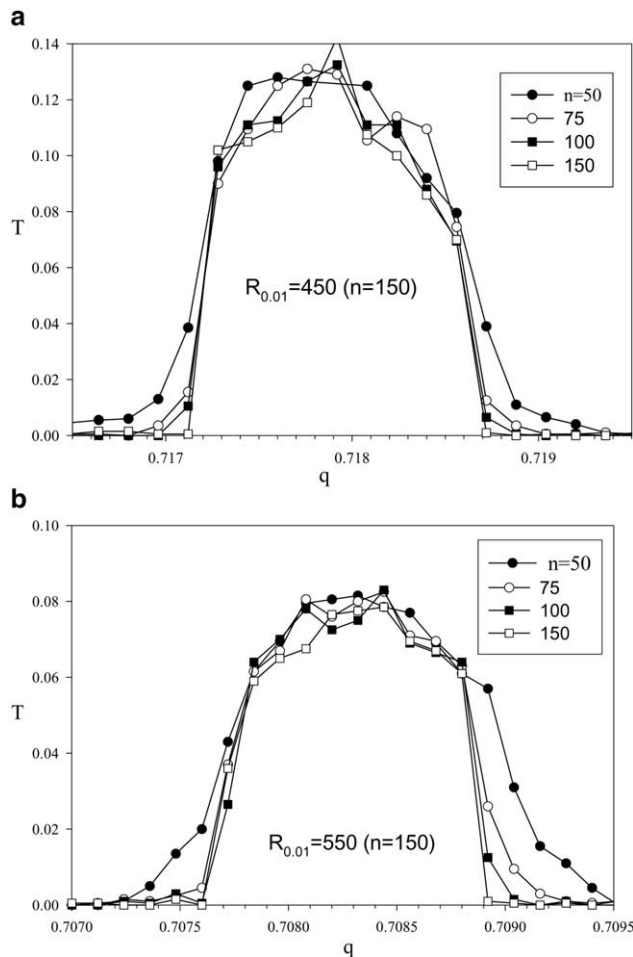


**Figure 11.** Peak shapes for different separation times  $n$  in a quadrupole field created with round rods with the ratio  $r/r_0 = 1.13$ . (a) Amplitude modulation of both the DC and RF voltages with  $m = 0.06$ ,  $\nu = 1/11$ , scan line  $a = 2\lambda q$  with  $\lambda = 0.17213$  which crosses the  $\beta_x$  boundaries of the stability island. (b) Amplitude modulation of the RF voltage only, stability island with  $m = 0.06$  and  $\nu = 1/12$ .  $\lambda = 0.1769$ . Operation at the upper tip.

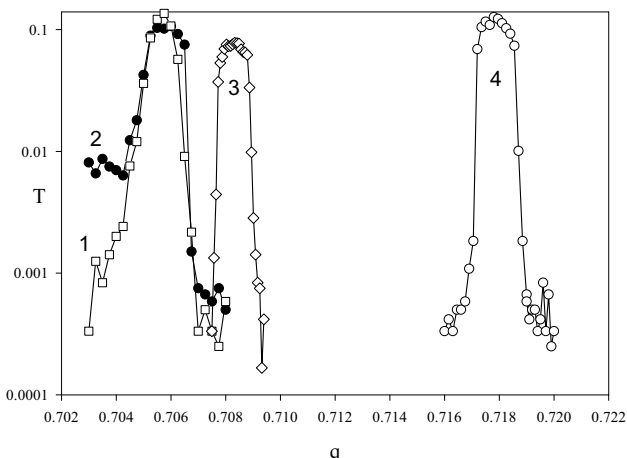


**Figure 12.** Comparison of peak shapes for different separation modes ( $n = 100$ ,  $N = 12,000$ ). Curve 1—perfect quadrupole field without modulation,  $\lambda = 0.1677$ ; curve 2—round rods with  $r/r_0 = 1.13$ , without modulation; curve 3—round rods with  $r/r_0 = 1.130$ ) with amplitude modulation of the RF voltage ( $m = 0.06$ ,  $\nu = 1/12$ , upper tip,  $\lambda = 0.1769$ ); curve 4—round rods with  $r/r_0 = 1.13$  with amplitude modulation of both the DC and RF voltages ( $m = 0.06$ ,  $\nu = 1/11$ ,  $\lambda = 0.17213$ ).

fringing field should be about  $n_z = 2$  or more RF cycles [16, 17]. Thus the axial ion velocity should be equal to

$$v_z \geq \frac{1.5r_0f}{2} = \frac{3}{4}r_0f \quad (13)$$

and the axial ion energy is equal to

$$E_z = \frac{1}{2}m\left(\frac{3}{4}r_0f\right)^2 \quad (14)$$

From eqs 11 and 14 we can calculate that  $(L/r_0) \geq 3n/4$  and  $L_m/L_q \leq 1/2$  at equal field radius field  $r_0$ , where  $L_m$  and  $L_q$  are required rod lengths with modulation and without modulation. Thus using trapping voltage modulation allows decreasing the rod length, for example, from 200 mm to 100 mm. As a result the cost of fabricating a rod set may be decreased.

Reducing the time required for ion separation may be useful in tandem mass spectrometry to enlarge the range of ion energies in reactions of ions with a gas target, or in applications like ICP-MS where the source produces ions with a relatively large energy spread. From the simulation data here we believe that the simplest method to improve performance is to operate at the tips of an island, created by RF modulation, at a low frequency ratio  $\nu = 1/10–12$  and with a modulation parameter  $m = 0.04–0.10$ .

## Acknowledgments

The authors gratefully acknowledge Professor Don Douglas for help in editing the manuscript.

## References

- March, R. E. Quadrupole Ion Trap Mass Spectrometry: A View at the Turn of the Century. *Int. J. Mass Spectrom.* **2000**, *200*, 285–312.
- Vedel, F.; Vedel, M.; March, R. E. New Schemes for Resonant Ejection in RF Quadrupolar Ion Traps. *Int. J. Mass Spectrom. Ion Processes* **1990**, *99*, 109–121.
- Alfred, R. L.; Londry, F. A.; March, R. E. Resonance Excitation of Ions Stored in a Quadrupolar Ion Trap. Part IV. Theory of Quadrupolar Excitation. *Int. J. Mass Spectrom. Ion Processes* **1993**, *1*, 171–185.
- Sheretov, E. P.; Gurov, V. S.; Kolotilin, B. I. Modulation Parametric Resonances and Their Influence on Stability Diagram Structure. *Int. J. Mass Spectrom.* **1999**, *184*, 207–216.
- Sudakov, M.; Konenkov, N.; Douglas, D. J.; Glebova, T. Excitation Frequencies of Ions Confined in a Quadrupole Field with Quadrupolar Excitation. *J. Am. Soc. Mass Spectrom.* **2001**, *11*, 11–18.
- Collings, B. A.; Douglas, D. J. Observation of Higher Order Quadrupole Excitation Frequencies in Linear Ion Trap. *J. Am. Soc. Mass Spectrom.* **2000**, *11*, 1016–1022.
- Kozo,, M. Quadrupole Mass Spectrometer, U.S. patent 5,227,692; July 13, 1993.
- Konenkov, N. V.; Sudakov, M. Y.; Douglas, D. J. Matrix Methods for the Calculation of Stability Diagrams in Quadrupole Mass Spectrometry. *J. Am. Soc. Mass Spectrom.* **2002**, *13*, 597–613.
- Konenkov, N. V.; Cousins, L. M.; Baranov, V. I.; Sudakov, M. Y. Quadrupole Mass Filter Operation with Auxiliary Quadrupole Excitation: Theory and Experiment. *Int. J. Mass Spectrom.* **2001**, *208*, 17–27.
- Baranov, V. I.; Konenkov, N. V.; Tanner, S. D. QMF Operation with Quadrupole Excitation. In *Plasma Source Mass Spectrometry, the New Millennium*; pp Holland, G.; Tanner, S. D., Eds.; Royal Society of Chemistry: Cambridge, 2001; 63–72.
- Douglas, D. J.; Konenkov, N. V. Influence of the 6th and 10th Spatial Harmonics on the Peak Shape of a Quadrupole Mass Filter with Round Rods. *Rapid Commun. Mass Spectrom.* **2002**, *16*, 1425–1431.
- Glebova, T.; Konenkov, N. V. Quadrupole Mass Filter Transmission in Island A of the first Stability Region with Quadrupolar Excitation. *Eur. J. Mass Spectrom.* **2002**, *8*, 201–205.
- Douglas, D. J.; Sudakov, M. Y.; Konenkov, N. V.; Glebova, T. A. Spatial Field Harmonics of a Quadrupole Mass Filter with Round Rods. *J. Tech. Phys.* **1999**, *10*, 96–101.
- Hairer, E.; Norsett, S. P.; Wanner, G. *Solving Ordinary Differential Equations*; Moscow: Mir, 1990; p 512.
- Hunter, K. L.; McIntosh, B. J. An Improved Model of the Fringing Fields of a Quadrupole Mass Filter. *Int. J. Mass. Spectrom. Ion Processes* **1989**, *87*, 157–164.
- McIntosh, B. J.; Hunter, K. L. Influence of Realistic Fringing Fields on the Acceptance of a Quadrupole Mass Filter. *Int. J. Mass. Spectrom. Ion Processes* **1989**, *87*, 165–179.
- Dawson, P. H. Source Analyzer Coupling in the Quadrupole Mass Filter. *Int. J. Mass Spectrom. Ion Processes* **1990**, *100*, 41–50.